# On the computation of wavenumber integrals in phase-shift migration of common-offset sections

Xinxiang Li and Gary F. Margrave


## ABSTRACT

The evaluation of wavenumber integrals often occurs in migration and modelling algorithms in exploration seismology. The integrals over offset-wavenumbers in phase-shift migration of common-offset sections are the specific case analysed in this paper. The accurate algorithm is numerically simple and easy to implement, but it is computationally very time consuming.

Two approximation methods to compute the offset-wavenumber integrals are discussed in this paper. The first method is the stationary-phase method, which is very often used to evaluate the offset-wavenumber integrals. The second method is called the trapezoidal Filon method, which has been known in synthetic seismogram theory for decades.

Numerical results from these two methods suggest that the stationary-phase method has high accuracy when the wavefield extrapolation depth step-size is not very small relative to the source-receiver offsets of the input common-offset sections. The trapezoidal Filon method, on the other hand, is more suitable in the evaluation of offset-wavenumber integrals when the offsets are large relative to the depth step-size.


## INTRODUCTION

Migration from separated offset sections has many advantages in seismic data analysis and interpretation over conventional prestack migration schemes. One of such advantages is the relative insensitivity to migration velocity errors, which has been used to perform migration velocity analysis and obtain stacked image by simple moveout correction on the image gathers (Sattlegger et al (1980), Deregowski (1990), Kim and Krebs (1993), and Ferber (1994)). Another advantage of common-offset-section migration is that it provides reflectivity information with preservation of changes in the offset direction, which is desired for AVO or AVA analysis (Ekren and Ursin, 1995, 1999). AVO or AVA analysis after migration is a topic drawing more and more attentions (Mosher et al., 1996 and Tygel et al., 1999).

Most of the earlier work on migration from common-offset sections utilised diffraction-summation type migration operators because of their independence of the acquisition geometry. However, because diffraction summation methods have difficulties to preserve the amplitude (reflectivity) information (among other reasons), Fourier domain methods are still attractive. A scheme of common-offset-section phase-shift migration, which involves offset-wavenumber integrals, was discussed by Popovici (1994) and then extended by Alkhalifah (1997) to a time migration for anisotropic media. The strategies of the evaluation of the offset-wavenumber integrals in Popovici (1994) and Alkhalifah (1997) are the same in that they both use the stationary-phase approximation method. The main difference between these evaluation techniques lies in the different methods employed in finding the

stationary-phase point. Popovici (1994) uses a numerical algorithm to find the root (zero value point) of the phase derivative function, and this algorithm is still expensive. Alkhalifah (1997) uses an algorithm to find the maximum of the phase function. By his own assessment, Alkhalifah's algorithm takes about 10% more computation time to migrate a single offset section than the time required by the conventional zero-offset phase-shift method.

In this paper, detailed numerical experiments with the stationary-phase method for the approximation of the offset-wavenumber integrals will be conducted. In cases when offsets are large relative to the wavefield extrapolation step-size, the stationary-phase approximation results in significant errors. Fortunately, in these cases, the trapezoidal Filon method becomes appropriate. The Filon method is analysed, and suggested when high accuracy is required for large offsets.

## THE INVOLVED OFFSET-WAVENUMBER INTEGRALS

Following the procedure of phase-shift migration scheme from common-offset sections, as presented in Popovici (1994) and Li and Margrave (1999), an integral over offset-wavenumber (denoted as $k_h$) needs to be evaluated for given values of:

the wavefield extrapolation depth step-size (denoted as $z$),

the temporal frequency (denoted as $\omega$),

the wavenumber value in the CDP direction (denoted as $k_x$),

the half source-receiver offset (denoted as $h_0$) of the input section, and

the relevant migration velocity (denoted as $v$).

The integral can be explicitly written as

$$\int \exp\left( iz\left[ \sqrt{\frac{\omega^2}{v^2} - \left(\frac{k_x - k_h}{2}\right)^2} + \sqrt{\frac{\omega^2}{v^2} - \left(\frac{k_x + k_h}{2}\right)^2} \right] - ik_h h_0 \right) dk_h = \int e^{i\phi(k_h)} dk_h , \qquad (1)$$

where $i$ is the square root of $-1$. The direct discritization of this equation results in a summation method of the evaluation of the integral as

$$\int e^{i\phi(k_h)} dk_h \approx \sum_j e^{i\phi(k_h(j))} \Delta k_h . \qquad (2)$$

The integral limits in (1) and the summation limits in (2) are set to (theoretically) include all the relevant $k_h$ values. However, in practice, the limits are often referred to the $k_h$-range in which the two square roots in equation (1) are both real, i.e., the $k_h$-range is determined by the following two inequalities:

$$|k_x - k_h| \cdot v \le 2|\omega| , |k_x + k_h| \cdot v \le 2|\omega| , \qquad (3a)$$

which is equivalent to one condition

$$|k_h| \le \frac{2|\omega|}{v} - |k_x| . \tag{3b}$$

This limitation (3b) of $k_h$ is used throughout this paper except otherwise expressed explicitly.

The direct summation method in equation (2) is considered accurate for the evaluation of the integral in equation (1) throughout this paper. The accuracies of the stationary-phase method and the trapezoidal Filon method are analysed by comparing these two methods with the direct summation method.

## STATIONARY-PHASE METHOD

The integrals for which the stationary-phase method was originally developed have the following general form (Murray, 1984, and Popovici, 1994):

$$f(\lambda) = \int_a^b g(t) e^{i\lambda h(t)} dt , \tag{4}$$

where $a$, $b$, $g(t)$, $h(t)$, $t$ and $\lambda$ are all real. As $\lambda$ tends to infinite, this integral can be approximated by

$$I_{SP} = g(t_0) \sqrt{\frac{2\pi}{\lambda |h''(t_0)|}} \cdot e^{i\left[\lambda h(t_0) + sign(h''(t_0))\pi/4\right]} . \tag{5}$$

This expression assumes that function $h$ has only one turning point (a relative maximum or minimum), at $t=t_0$, in the integration range ($a$, $b$), which means that

$$h'(t_0) = 0 , \; h''(t_0) \neq 0 \;\text{ and }\; a < t_0 < b . \tag{6}$$

This approximation will be referred as $I_{SP}$ in this paper for simplicity.

If there are more than one turning point in the interval ($a$, $b$), integral (4) can be simply evaluated by splitting the integral range into one-turning-point segments.

One special case is that one of the integral limits, $a$, for example, may be the only turning point in the integral range. In this case the integral (4) can then be approximated by a half of the value of $I_{SP}$ in (5) (Murray, 1984), and it is called the half $I_{SP}$ approximation.

The stationary-phase $I_{SP}$ approximation for the specific wavenumber integral in equation (1) can be written directly from (5) as

$$I_{SP} = \sqrt{\frac{2\pi}{|\phi''(k_{h0})|}} \cdot e^{i\left[\phi(k_{h0}) + sign(\phi''(k_{h0}))\pi/4\right]} \tag{7}$$

with $\lambda=1$, $g=1$, and $h=\phi$, and integral variable being $k_h$ instead of $t$. The value $k_{h0}$ is the stationary point in the integral range. For offset-wavenumber integral in equation (1), there can only be one turning point because the second order derivative of

function $\phi(k_h)$ is non-zero in the whole $k_h$-range where the integral is evaluated. Explicitly, the second derivative can be expressed as

$$\frac{-\frac{z}{4}}{\sqrt{\frac{\omega^2}{v^2}-\left(\frac{k_x-k_h}{2}\right)^2}}+\frac{-\frac{z}{4}}{\sqrt{\frac{\omega^2}{v^2}-\left(\frac{k_x+k_h}{2}\right)^2}}+\frac{-\frac{z}{4}(k_x-k_h)^2}{4\cdot\left\{\frac{\omega^2}{v^2}-\left(\frac{k_x-k_h}{2}\right)^2\right\}^{\frac{3}{2}}}+\frac{-\frac{z}{4}(k_x+k_h)^2}{4\cdot\left\{\frac{\omega^2}{v^2}-\left(\frac{k_x+k_h}{2}\right)^2\right\}^{\frac{3}{2}}}, \tag{8}$$

which is a summation of four terms with the same sign (see also Popovici, 1994).

From expression (7), the evaluation of the integral in equation (1) over a certain range of $k_h$ is reduced to a problem by using the values of $\phi$ and $\phi''$ at only one $k_h$-location, at which the derivative $\phi'$ becomes zero. Although $\phi'$ can be explicitly expressed as a function of $k_h$, there is no straightforward algorithm to find its zero point (Popovici, 1994). Another way to locate the stationary-phase point (zero point of $\phi'$) is to find where the function $\phi$ yields its maximum value (Alkhalifah, 1997).

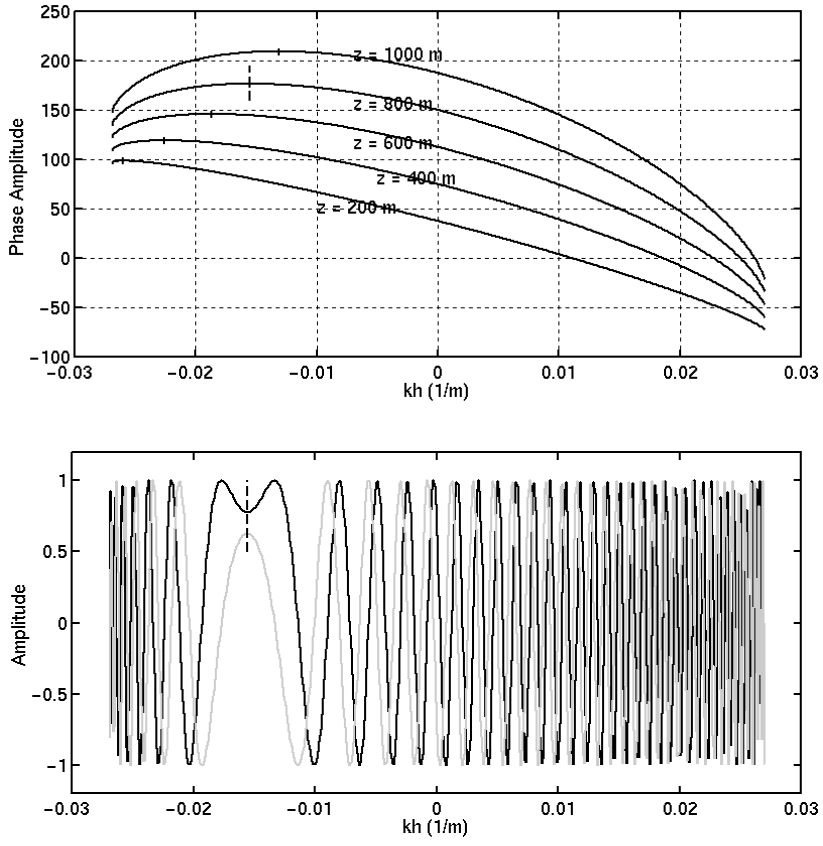


Figure 1. (a) shows several curves of $\phi$ as functions of $k_h$ with different z value and all other related quantities are fixed. Only the dark line's turning point is indicated. (b) shows the real part (the dark curve) and the imaginary part (light grey curve) of $exp(i\phi)$ (corresponding to the dark line in (a)). The stationary-phase point in (b) is indicated with a vertical dashed line.

Figure 1 (a) shows some examples of the phase function $\phi$ for different depth steps and offsets. The turning points are indicated with little vertical lines. Figure 1 (b) shows the real part (dark curve) and the imaginary part (grey line) of one of the integrands, $exp(i\phi)$, and the stationary-phase point is also indicated with a dashed vertical line. (The turning point of $\phi$ and the stationary-phase point of $exp(i\phi)$ always represent the same thing in this paper.)

Figure 1 (b) demonstrates why the integral of the exponential function $exp(i\phi)$ over the $k_h$ range is mainly determined by the behaviour of the function $\phi$ (and its derivatives) at the turning point. The integrand, $exp(i\phi)$, oscillates rapidly between –1.0 and 1.0 at all $k_h$ locations except the ones close to the stationary-phase point. The oscillatory values cancel each other out during the integration, and the main contribution to the integral comes from the points close to the stationary-phase point.

## SHORTCOMINGS OF STATIONARY-PHASE METHOD TO EVALUATE OFFSET-WAVENUMBER INTEGRALS

In general, the stationary-phase method has plausible accuracy for the approximation of the offset-wavenumber integral expressed in equation (1). However, attention should be paid in cases when the approximation accuracy may not be satisfactory.

The stationary-phase point tends to one of the integral-limits determined by (3b) when $z$ is relatively small respect to $h_0$. The asymptotic stationary-phase point is the $k_h$ value where one of the square roots in (1) equals zero. This can be seen by examining the first order derivative of $\phi$, which is

$$\phi'(k_h) = z \cdot \left[ \frac{k_h + k_x}{\sqrt{\frac{\omega^2}{v^2} - \left(\frac{k_h + k_x}{2}\right)^2}} + \frac{k_h - k_x}{\sqrt{\frac{\omega^2}{v^2} - \left(\frac{k_h - k_x}{2}\right)^2}} \right] - h_0 \,. \qquad (9)$$

When the ratio $h_0/z$ tends to be large, the value of the summation inside the bracket has to be large at the turning point to ensure $\phi'$ to be zero at the turning point. Therefore, the stationary-phase point, i.e., the turning point, tends to be the $k_h$ value where one or both of the square-root terms in the bracket yield very small values.

In practice, when the velocity vertical variation is significant (even without considering lateral velocity variation), wavefield extrapolation with appropriate accommodation of the velocity variation usually limits the depth step to a much smaller size relative to the offset range. In such cases, the stationary-phase point in the non-evanescent region of $k_h$ is very close to the critical point. In addition, the offset-wavenumber is always sampled with a certain increment, and very often the stationary-phase point cannot be very well separated from the critical point. Figure 2 shows some curves of $\phi$ for different step size $z$'s, in a half-offset range of 0 to 2000 m. The stationary-phase points of all the curves are indicated by "+" symbols.

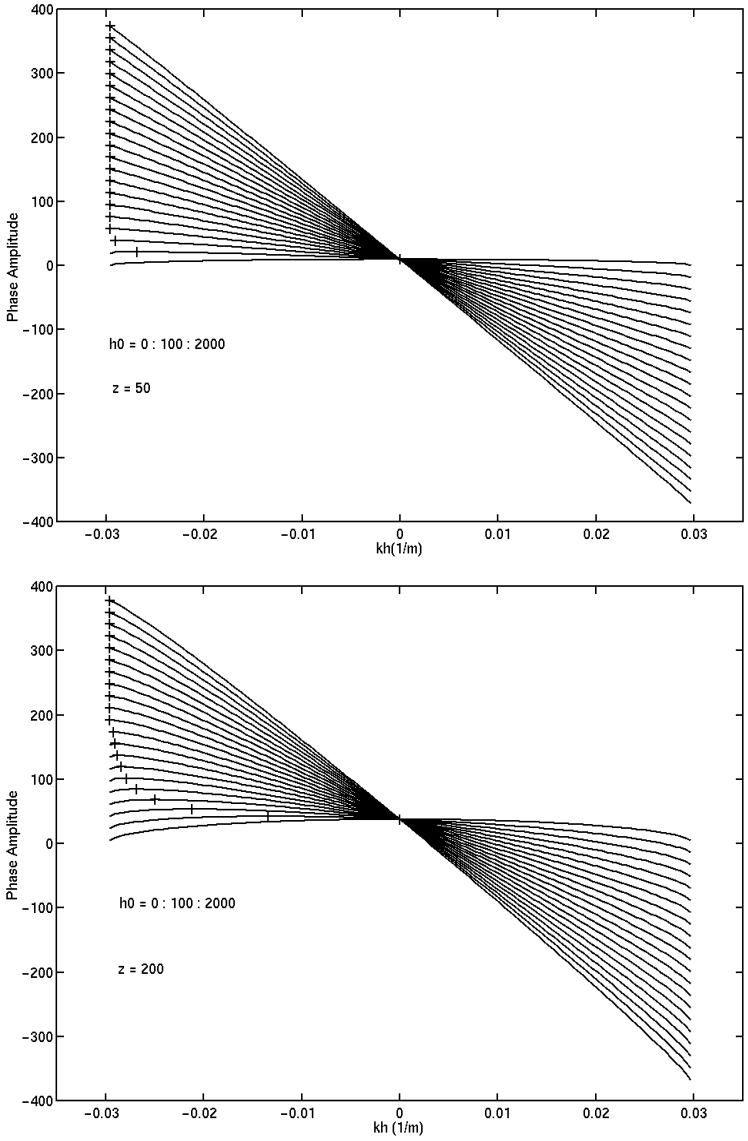


Figure 2. Curves of $\phi$ for different values of $h_0$, which is sampled from 0 to 2000 m with 100 m increment, where (a) shows curves with $z$ = 50 m and (b) the curves with $z$ = 200 m. All the other quantities are fixed at the same values for all the curves.

In Figure 2, many of the stationary-phase points are practically (numerically) at the integral limit point. This results in integration values that are closer to the half $I_{SP}$ approximation instead of the full $I_{SP}$ approximation. Some experiments with $I_{SP}$ and half $I_{SP}$ are shown Figure 3, where the approximation errors of the $I_{SP}$ and the half $I_{SP}$ are plotted. The half $I_{SP}$ is a better approximation when the stationary-phase points tend to one of the integral limits.

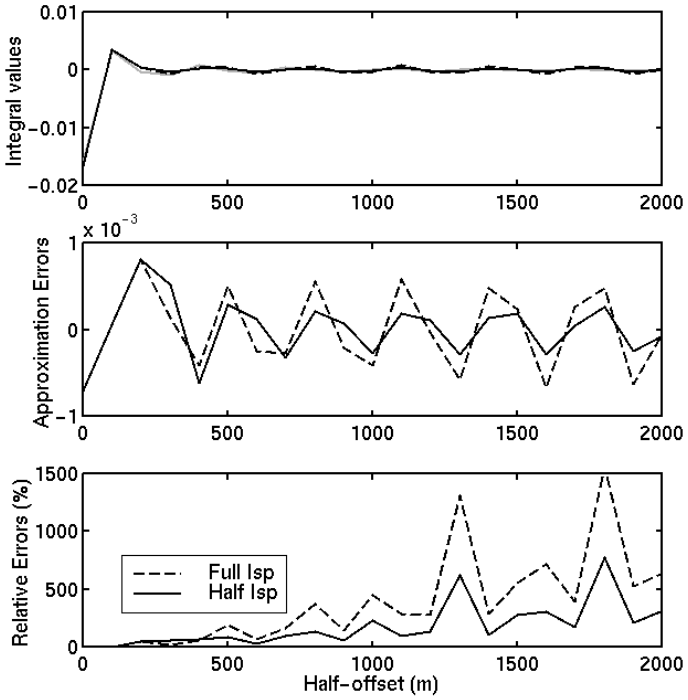


Figure 3. Approximations of stationary-phase method using full $I_{SP}$ and half $I_{SP}$ approximations. (a) shows three curves corresponding to real parts of accurate values (grey line), $I_{SP}$ values (dashed dark line) and half $I_{SP}$ values (dark solid line) for different $h_0$ values (from 0 to 2000 m) and fixed z = 50 m; (b) is the approximation errors (real part only) of $I_{SP}$ (dashed line) and half $I_{SP}$ (solid line); and (c) is the absolute error of $I_{SP}$ (dashed line) and half $I_{SP}$ (solid line) relative to the absolute accurate values.

In Figure 3(a), it seems that both the $I_{SP}$ and half $I_{SP}$ approximations are quite good because no evident visual deviations can be recognised from the three curves. In fact, even the approximation errors, as shown in Figure 3(b), are all small numbers, the approximations are unacceptable because the relative errors, as shown in Figure 3(c), are "wildly" large. With relative errors greater than 100%, some of the $I_{SP}$ and half $I_{SP}$ approximations involve more errors than simply taking zero as the integral values. A conclusion can be drawn from the results in Figure 3 that when depth-step $z$ is small relative to the half-offset value $h_0$, the stationary-phase method should not be used to evaluate the offset-wavenumber integrals expressed in (1).

For example, when $z$ = 50 m and $h_0$ = 400 m, the stationary-phase point is very close to the integral limit (Figure 4(a)), and the integrand is basically oscillatory throughout the whole integral range. The oscillatory curve shown in Figure 4(b) is the real part of the integrand function $exp(i\phi)$. Practically speaking, the phase is not very "stationary" at the stationary-phase point in this example, and the contribution from the local values of the integrand around the stationary-phase point does not dominate as much as it does for an integrand function shown in Figure 1(b).

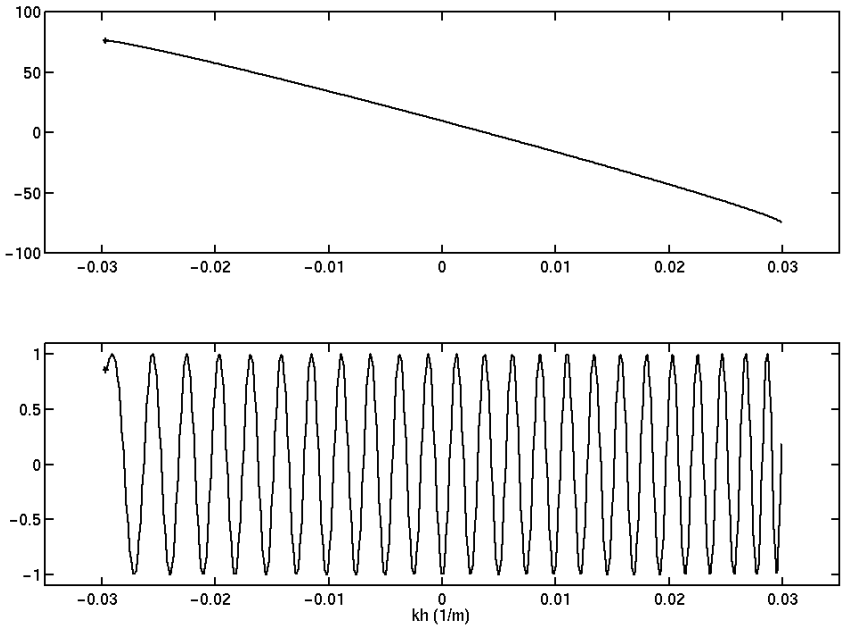


Figure 4. Function $\phi$ (a) and $exp(i\phi)$ (real part only) (b) for z=50 m and $h_0$=400 m. Other quantities are the same as in Figure 3. In this case, the stationary-phase point is close to the $k_h$ integral limit.

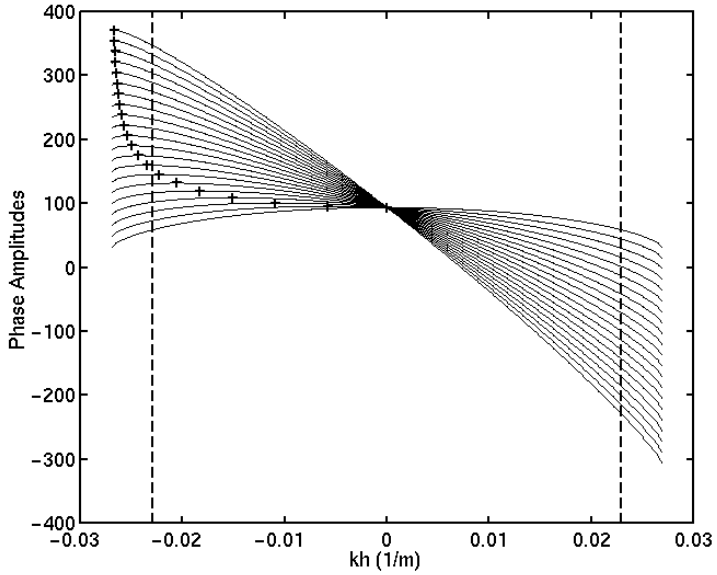


Figure 5: Migration dip-limits limit the offset-wavenumber integral to a smaller range and often make the stationary-phase point lying outside the integral range. The solid-line curves are drawn for 90-degree dip limit, the two vertical dashed-lines indicate the integral range determined by a 60-degree dip-limit. Many of the stationary-phase points (plotted with markers "+") lie outside the narrower integral range. In this figure, $z$ is fixed at 500 m, and $h_0$ ranges from 0 to 2000 m. It can be seen that all the approximations for 90-degree dip-limit cases are very accurate, while the approximations for 60-degree cases become unacceptable when $h_0$ is greater than 500 m. Further more, when $h_0$ is greater than 900 m, simply setting the integral value to be zero gives better approximations.

For many practical reasons, migration algorithms often involve dip limits. As mentioned above, the widest range of the $k_h$-integral (1) is determined by the $k_h$ values where the wave-components related to these $k_h$-values (and given $k_x$ and $\omega$) are becoming evanescent. A migration dip-limitation of less than 90 degrees limits $k_h$ to even narrower ranges. In such cases, the stationary-phase points may often reside outside the integral range even for not very large $h_0/z$ ratio. An example with 60-degree dip-limit is shown in Figure 5 where $z$ = 500 m and $h_0$ ranges from 0 to 2000 m. This involves more difficulties for applying stationary-phase approximation to the offset-wavenumber integrals, or more strictly, the stationary-phase approximation is not valid any more. The approximation results are shown in Figure 6.

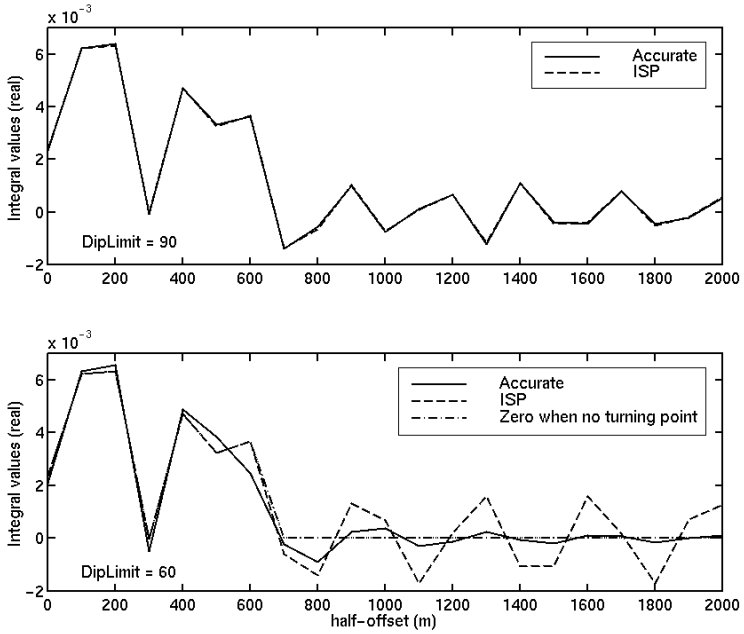


Figure 6: Stationary-phase approximations for 90-degree (a) and 60-degree (b) dip limits.

Fortunately, in cases where $h_0/z$ is relatively large, $\phi$ as a function of $k_h$ is (at least piecewisely) close to a straight line, i.e., $\phi \sim -h_0 k_h$, which can be seen graphically from the curves in Figure 2. This piecewise linear approximation of the function $\phi$ satisfies the conditions of the trapezoidal Filon method for the evaluation of wavenumber integrals.

## TRAPEZOIDAL FILON METHOD

The trapezoidal Filon method (Frazer, 1988) is an approximation algorithm to evaluate an integral with a general form of

$$\int_{\Gamma} f(p) e^{sg(p)} dp \,. \tag{10}$$

If the two functions $f$ and $g$ can be approximated piecewisely as linear function, then trapezoidal Filon method provides an approximation of the integral (10) as

$$\sum \int_{p_1}^{p_2} f(p) e^{sg(p)} dp = \sum \left\{ \frac{\delta(p)}{s\delta(g)} \left[ \delta\left(f e^{sg}\right) - \frac{\delta(f)\delta\left(e^{sg}\right)}{s\delta(g)} \right] \right\}, \tag{11}$$

where $\delta(p) = p_2 - p_1$, and $\delta(u) = u(p_2) - u(p_1)$ with $u$ representing any function of $p$ ($f$, $e^{sg}$ and $g$). The summation is over all the pieces (segments of $p$) on which both $f$ and $g$ can be approximated by straight lines. Equation (11) is called the trapezoidal Filon approximation.

For the integral expressed in equation (1), the variable $p$ becomes $k_h$, the function $f$ takes the constant value *1*, and $g$ is equal to $\phi$. The constant $s$ is simply the square root of $-1$. The trapezoidal Filon approximation (11) becomes

$$\sum \int_{k_{h1}}^{k_{h2}} e^{i\phi(k_h)} dk_h = \sum \left\{ \frac{\delta(k_h)}{i\delta(\phi)} \delta\left(e^{i\phi}\right) \right\}, \tag{12}$$

and the only condition for the approximation is that function $\phi$ can be approximated by linear function within each and every $k_h$-segment ($k_{h1}$, $k_{h2}$).

If possible, different sizes of interval ($k_{h1}$, $k_{h2}$) within the integral range should be more efficient. However, determining the length of each ($k_{h1}$, $k_{h2}$) raises another problem and may also require more computation time. For simplicity, the following analysis of the Trapezoidal Filon method is based on equal-size intervals throughout the whole integral range.

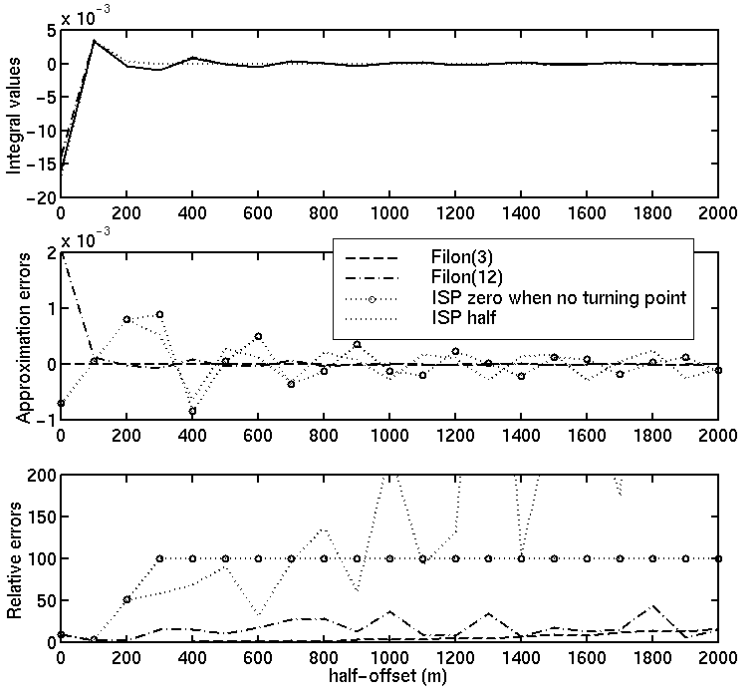


Figure 7. Trapezoidal Filon and stationary-phase approximations with depth step $z$ = 50 m and the half-offset $h_0$ ranging from 0 to 2000 meters. (a) shows the integral values evaluated by the accurate method, two Filon approximations and the stationary-phase approximation. (b) shows the approximation errors of these methods and (c) shows the relative errors in percentage of the accurate values.

For depth step $z$ = 50 m, which was used for the results shown in Figure 3 and Figure 4, two different interval size Filon approximation results are shown in Figure 7 with comparisons with the results from accurate method and the stationary-phase method. In Figure 7 (a), the integral values from different methods are shown together, and no significant difference can be seen. In Figure 7 (b), on the other hand, the approximation errors relative to the accurate values show that the two Filon approximations are better than the stationary-phase approximations. The symbol "Filon (3)" indicates the results computed using the Filon method with linear-function approximation for every 3 consecutive $k_h$ samples, while "Filon (12)" stands for the use of the Filon method with linear-function approximation for every 12 consecutive $k_h$-samples. Figure 7 (c) shows the relative errors of the three approximations. Note that the Filon approximations have much better stability at large offsets.

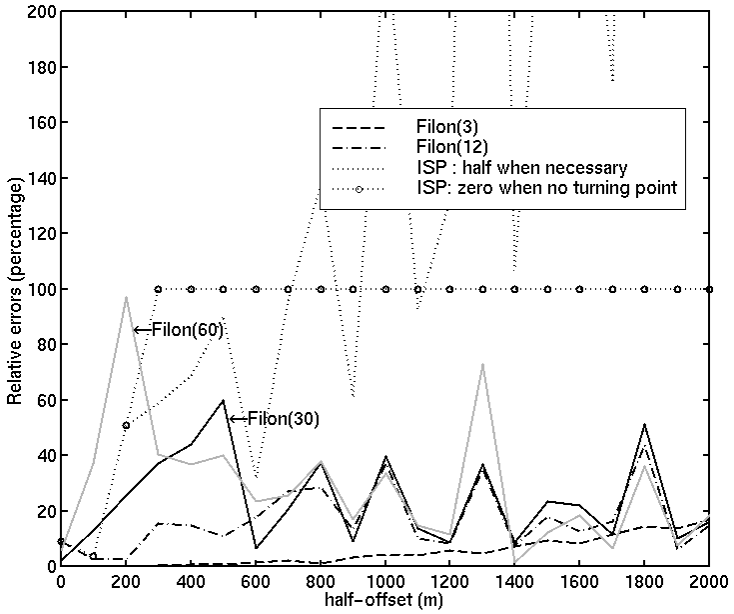


Figure 8. The relative errors represented as percentages of the absolute values of the approximation errors (which are complex values) over the absolute values of the accurate results (complex too).

Figure 8 represents the relative errors of the Filon approximations with four different interval sizes, which are denoted as "Filon (3)", "Filon (12)", "Filon (30)", and "Filon (60)". The results in this figure are obtained with $z$ = 20 m, which is more likely the size practically used for wavefield extrapolation with strong vertical variation. For comparison, the stationary-phase approximations are shown as the dotted lines. Note that the stationary-phase approximations are not acceptable in this case, especially for large offsets.

## EFFICIENCY COMMENTS

Although the main purpose in experimenting with different approximation algorithms is to find a method with less computation cost, the accuracy should always be a concern. The above analysis concentrates on the ability of the stationary-phase and the trapezoidal Filon methods to provide acceptable approximations of the offset-wavenumber integrals expressed in equation (1). The experiment codes were all

implemented in Matlab, and they may not be optimised. However, the following table of floating-point operations counted by Matlab function "flops" for different methods should still provide an intuitive indication of how fast or slow an algorithm might be. These operations do not include the evaluation of $\phi$ as a function of $k_h$, which takes time especially for the direct summation method.

Table 1: Number of floating point operations for different algorithms

| **Methods** | **Number of operations** |
|---|---|
| Accurate summation | 9559 |
| Stationary-phase | 671 |
| Filon (3) | 14959 |
| Filon (12) | 2759 |
| Filon (30) | 1059 |
| Filon (60) | 559 |
| Filon (100) | 359 |

Another efficiency aspect of these methods is the number of $k_h$-samples where the function $\phi$ and/or its derivatives need to be evaluated. Basically, the stationary-phase method needs the values of $\phi$ and its second derivative at only one sample (the stationary-phase point). The computation cost of stationary-phase method is the time used to find the stationary-phase point, which can be expensive. For the trapezoidal Filon method, the cost is directly related to the interval size where the linear function is used to approximate the function $\phi$. Longer interval results in a faster algorithm, but provides less accuracy.

Note that in Figure 8, Filon (60) provides better approximation, except at $h_0 = 0$, 100 and 200 m, and uses less operations than the stationary-phase method as shown in Table 1.

## MULTI-STEP WAVEFIELD EXTRAPOLATION

In practical implementation of phase-shift migration algorithm, the wavefield at any depth may be directly obtained by a multi-step extrapolator, such as the nonstationary migration filters in the v(z) f-k algorithm (Margrave, 1998, Li and Margrave, 1998). In these cases, the offset-wavenumber integral can be written as

$$\int exp\left( i\int_0^z \left[ \sqrt{\frac{\omega^2}{v(z')^2} - \left(\frac{k_x - k_h}{2}\right)^2} + \sqrt{\frac{\omega^2}{v(z')^2} - \left(\frac{k_x + k_h}{2}\right)^2} \right] dz' - ik_h h_0 \right) dk_h = \int e^{i\phi(k_h)} dk_h . \quad (13)$$

Here the function $\phi$ and its derivatives may not have analytical expressions, such as equations (8) and (9). Therefore, the application of the stationary-phase approximations may require numerical evaluation of the function $\phi$ and its derivatives. This may involve some more computation cost than the single-step wavefield extrapolator may. However, the step-size (still denoted as $z$) in equation (13) practically is much larger than the single depth step in equation (1), and the $z$-to-$h_0$ ratio is no longer a problem except for the image of very shallow layers. As shown in Figure 6(a), where $z$ = 500 m and $h_0$ ranges from 0 to 2000 m, the stationary-phase approximation has very high accuracy when migration dip limit is not an issue.

## CONCLUSIONS

This paper presents some numerical results of the evaluation of the offset-wavenumber integrals involved in phase-shift migration of common-offset sections. The stationary-phase method may not be appropriate when wavefield extrapolation depth step is small relative to the offset values, although it has been used by many authors to approximate these integrals. It also shows that even when step size is not small, migration dip limit may also introduce difficulties for applying stationary-phase method. The experiments on the trapezoidal Filon method show that in the cases where the stationary-phase method failed to provide accurate approximations, the Filon method may be a better choice. The cost of trapezoidal Filon method can be comparable to stationary-phase method, and might be even faster.

The stationary-phase approximation of an integral of some wavenumber function depends on the values of the function at locations close to the stationary phase point. This implies that the values of the function at locations far away from the stationary-phase point are not taken into account at all. Our experiments and the results of other authors (e.g., Popovici, 1994) show that stationary-phase approximation method has very high accuracy except for very small depth step. Multi-step extrapolation scheme, equation (13), can practically overcome the small depth-step extrapolation problem except the very shallow part of the imaging results.

## FUTURE WORK

Many authors found that the practical computation time may most be spent on searching the stationary-phase point. We propose another way to use stationary-phase method. That is, instead of locating the stationary-phase point itself, we could find a much smaller integral range which includes the stationary-phase point, and then calculate the integral only over this smaller range accurately. There should be faster methods to find such smaller ranges rather than to locate the stationary-phase point.

## REFERENCES

Alkhalifah, Tariq, 1997, Prestack time migration for anisotropic media: 67th Annual Internat. Mtg., Soc. Expl. Geophys., Expanded Abstracts, 1583-1586.

Deregowski, S. M., 1990, Common-offset migrations and velocity analysis: First Break, 8, no. 6, 224-234.

Ekren, Bjorn O. and Ursin, Bjorn, 1995, Frequency-wavenumber constant-offset migration and AVO analysis: 65th Annual Internat. Mtg., Soc. Expl. Geophys., Expanded Abstracts, 1377-1380.

Ekren, Bjorn O. and Ursin, Bjorn, 1999, True-amplitude frequency-wavenumber constant-offset migration: Geophysics, 64, 915-924.

Ferber, R.-G., 1994, Migration to multiple offset and velocity analysis: Geophys. Prosp., 42, no. 2, 99-112.

Frazer, L. Neil, 1988, Quadrature of wavenumber integrals, III.3 in "Seismological Algorithms, Computational Methods and Computer Programs", Doornbos, D. J. (Ed.), Academic Press.

Frazer, L. Neil and Gettrust, Joseph F., 1984, On a generalization of Filon's method and the computation of the oscillatory integrals of seismology, Geophys. J.R. Astr. Soc., vol. 76, 461-481

Kim, Young C. and Krebs, Jerry R., 1993, Pitfalls in velocity analysis using common-offset time migration: 63rd Annual Internat. Mtg., Soc. Expl. Geophys., Expanded Abstracts, 969-973.

Li, X, and Margrave, G. F., 1998, Prestack v(z) f-k migration for PP and PS data, CREWES Research Report, Vol. 10.

Li, X, and Margrave, G. F., 1999, Prestack v(z) f-k migration from common-offset sections, CREWES Research Report, this volume.

Margrave, Gary F., 1998, Direct Fourier migration for vertical velocity variations: 68th Annual Internat. Mtg., Soc. Expl. Geophys., Expanded Abstracts, , 1712-1715.

Mosher, C. C., Keho, T. H., Weglein, A. B. and Foster, D. J., 1996, The impact of migration on AVO: Geophysics, 61, no. 06, 1603-1615.

Murray J.D., 1984, Method of stationary-phase, Chapter 4 of “Asymptotic Analysis”, Applied Mathematical Sciences Vol. 48, Springer-Verlag New York Inc.

Popovici, Alexander M., 1994, Reducing artifacts in prestack phase-shift migration of common-offset gathers: 64th Annual Internat. Mtg., Soc. Expl. Geophys, Expanded Abstracts, 684-687.

Sattlegger, J. W., Stiller, P. K., Echterhoff, J. A. and Hentschke, M. K., 1980, Common-offset plane migration (COPMIG): Geophys. Prosp., 28, no. 6, 859-871.

Tygel, M., Santos, L. T., Schleicher, J. and Hubral, P. 1999, Kirchhoff imaging as a tool for AVO/AVA analysis, The Leading Edge, August 1999, vol. 18, No. 8, 940-945.